cAMP-dependent Protein Kinase Induces cAMP-response Element-binding Protein Phosphorylation via an Intracellular Calcium Release/ERK-dependent Pathway in Striatal Neurons*

Patrizia Zanassi‡, Mayra Paolillo‡, Antonio Feliciello§, Enrico V. Avvedimento§¶, Vittorio Gallo‖, and Sergio Schinelli‡‖

From the ‡Dipartimento di Farmacologia Sperimentale ed Applicata, Facoltà di Farmacia, Università di Pavia, Pavia 27100, Italy, §Dipartimento di Biologia e Patologia Cellulare e Molecolare, Consiglio Nazionale delle Ricerche, Napoli 80131, Italy, ¶Dipartimento di Medicina Sperimentale, Facoltà di Medicina di Catanzaro, Università di Catanzaro, Catanzaro 88100, Italy, and ‖Laboratory of Cellular and Molecular Neurophysiology, NICHD, National Institutes of Health, Bethesda, Maryland 20892

Activation of the cAMP-dependent protein kinase A (PKA) pathway may induce cAMP-response element-binding protein (CREB) phosphorylation either directly or via cross-talk mechanisms with other signal transduction pathways. In this study, we have investigated in striatal primary cultures the mechanism by which activation of the cAMP/PKA-dependent pathway leads to CREB phosphorylation via the extracellular signal-regulated kinase (ERK)-dependent pathway. We have found that PKA-induced CREB phosphorylation and CREB-dependent transcription are mediated by calcium (Ca^{2+}) release from intracellular stores and are blocked by inhibitors of the protein kinase C and ERK pathways. This mechanism appears to be mediated by the small G-protein Rap1, whose activation appears to be primed by PKA-induced Ca^{2+} release but not further induced by direct or indirect PKA- or protein kinase C-dependent phosphorylation. These results suggest that, in striatal neurons, intracellular Ca^{2+} release, Rap1, and ERK pathway play a crucial role in the PKA-induced CREB phosphorylation and CREB-dependent transcription.

The dopaminergic striatal system is the main target of the antipsychotic agents used in the treatment of schizophrenia (1) and of the psychostimulant drugs cocaine and amphetamines (2). The prolonged administration of these drugs increases the synaptic availability of dopamine and induces many dopamine-dependent adaptive responses culminating in the transcription of striatal cAMP-response element (CRE)[1]-dependent genes, such as the immediate early gene c-*fos* and the neuropeptides dynorphin, substance P, and enkephalins.

CREB phosphorylation, initially thought to be mediated exclusively by the cAMP/protein kinase A (PKA) pathway (3), is also induced by Ca^{2+}-dependent signal transduction pathways. Two members of the Ca^{2+}/calmodulin-dependent kinase family (CaMK), CaMKII (4) and CaMKIV (5, 6), are activated by Ca^{2+} entry through an L-type voltage-sensitive Ca^{2+} channel or glutamate N-methyl-D-aspartic acid (NMDA) receptors (7) and induce CREB phosphorylation. Moreover, Ca^{2+} influx via L-type voltage-sensitive Ca^{2+} channel or α-amino-3-hydroxy-5-methylisoxazole-4-propionic acid receptors and the release of Ca^{2+} from intracellular stores, elicited by the stimulation of growth factors receptors, activate the extracellular signal-related protein kinase (ERK)/mitogen-activated protein kinase pathway and induce CREB phosphorylation via the ribosomal S6 kinase 2 in PC12 cells (8, 9), in primary neuronal cultures (10, 11), and in brain slices (12).

The ERK pathway plays a pivotal role in stimulus-dependent gene regulation in the central nervous system, because pharmacological manipulations of the ERK pathway functionality affect the synaptic plasticity mechanisms supposed to underlie learning and memory (13). The cascade responsible of the ERK pathway activation requires the stimulus-dependent recruitment of the small G protein Ras, which in turn activates the Raf and MEK kinases. Although Ca^{2+}-dependent activation of Ras has been demonstrated in several experimental models (14), in the central nervous system an alternative route to ERK activation via the cAMP/PKA- or Ca^{2+}-dependent pathway has been recently characterized. This route implies the participation of the small G protein Ras-related Rap1 and the downstream kinase B-Raf (15, 16).

The importance of the Rap1/B-Raf system in the cross-talk between the cAMP/PKA- and ERK-dependent pathways has received further attention by the recent identification of two novel families of Rap1GEF activated by direct binding to Ca^{2+} and cAMP (17). However, these results were obtained mainly in platelets and PC12 cells, rather than in primary neural cells, which might display distinct signal transduction pathways.

---

[1] The abbreviations used are: CRE, cAMP-response element; PKA, protein kinase A; CREB, cAMP-response element-binding protein; ERK, extracellular signal-regulated kinase; PKC, protein kinase C; CaMK, Ca^{2+}/calmodulindependent kinases; NMDA, N-methyl-D-aspartic acid; RSK, ribosomal S6 kinase; H89, N-[2-(p-bromocinnamylamino)ethyl]-5-isoquinolinesulfonamide; 8-CPT, 8-(4-chlorophenylthio)-adenosine 3′,5′-cyclic monophosphate sodium salt; PMA, phorbol 12-myristate 13-acetate; BAPTA-AM, 1,2-bis-(o-aminophenoxy)ethane-N,N,N′,N′-tetraacetic acid tetra-(acetoxymethyl)-ester; fura-2/AM, 1-[2-(5-carboxyoxazol-2-yl)-6-aminobenzo-furan-5-oxy]-2-(2′-amino-5′methylphenoxy)-ethane N,N-N′,N′-tetraacetic acid pentacetoxymethyl ester; PD98059, 2′-amino-3′-methylflavone; Gö6976, [12-(2-cyanoethyl)-6,7,12,13-tetrahydro-13-meth-

yl-5-oxo-5H-indolo[2,3-*a*]pyrrolo[3,4-*c*]carbazole]; APV, D-(−)-2-amino-5-phosphonopentanoic acid; GST-ral-RBD, GST fusion protein of the minimal Rap1-binding domain of ralGDS; MEK, mitogen-activated protein kinase/extracellular signal-regulated kinase kinase; TBS, Tris-buffered saline; TBSM, TBS containing 4% nonfat dry milk; MOPS, 3-(N-morpholino)propanesulfonic acid; P-CREB, phosphorylated Ser[133] CREB; P-ERK2, phosphorylated ERK2; GST, glutathione S-transferase.
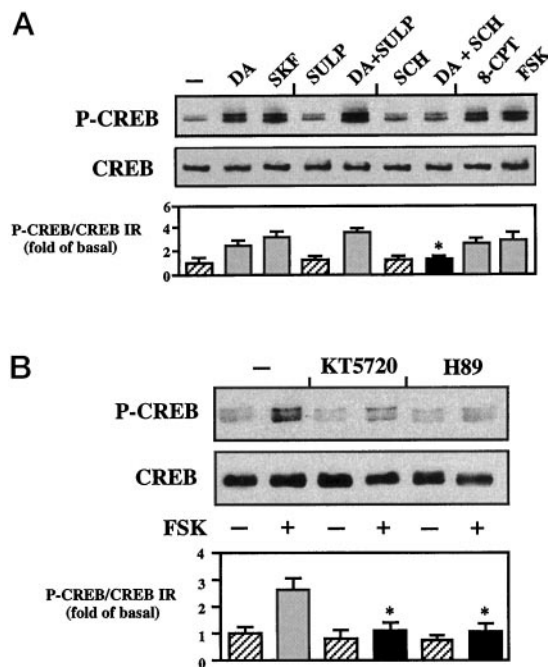
Intracellular Calcium Induces CREB Phosphorylation

A

B

FIG. 1. **Stimulation of D$_1$-like receptors and forskolin induce Ser^{133} CREB phosphorylation in primary striatal cultures.** *A*, cells were preincubated for 15 min with the D$_2$-like antagonist sulpiride (*SULP*, 100 μM) or the D$_1$-like antagonist SCH 23390 (*SCH*, 100 μM) and then left untreated (−) or stimulated for 10 min with dopamine (*DA*, 100 μM), with the D$_1$-like agonist SKF 38393 (*SKF*, 100 μM), with dopamine in the presence of sulpiride (*DA + SULP*), with dopamine in the presence of SCH 23390 (*DA + SCH*), with the membrane-permeable cAMP analogue 8-CPT (500 μM), and with the adenylylcyclase activator forskolin (*FSK*, 20 μM). *, $p < 0.05$ compared with dopamine. *B*, cells were preincubated with the PKA inhibitors KT5720 (10 μM) and H89 (20 μM) for 30 min and then left untreated (−) or stimulated (+) for 10 min with forskolin (*FSK*, 20 μM). *, $p < 0.05$ compared with forskolin. Nuclear protein extracts were then analyzed by Western blot with antibodies directed against CREB phosphorylated in Ser^{133} (P-CREB; *upper panel* in *A* and *B*) or against phosphorylation state-independent CREB (CREB, *lower panel* in *A* and *B*) to normalize for the total amount of CREB. Data are reported as P-CREB/CREB immunoreactivity (*IR*), and the average -fold increase (mean ± S.E.) over basal level is reported in the *bar graph* (*n* = 4).

Furthermore, the exact mechanism by which the cAMP/PKA-dependent pathway induces ERK activation and the role, if any, of Rap1 in CREB phosphorylation and CRE-dependent transcription have not yet been investigated.

In an attempt to address these questions, in this study we have investigated the mechanisms involved in cAMP/PKA-dependent ERK activation, CREB phosphorylation, and CRE-dependent gene transcription in striatal neurons.

EXPERIMENTAL PROCEDURES

Materials—The antibodies directed against phosphorylated Ser^{133} CREB (P-CREB) and phosphorylation state-independent CREB were purchased from Upstate Biotechnology, Inc. (Lake Placid, NY). The antibodies directed against dually phosphorylated ERK (Thr^{202} and Tyr^{204}) and phosphorylation state-independent ERK were from New England Biolabs (Beverly, MA); those against Rap1, B-Raf, and the protein-tyrosine kinase PYK2 were purchased from Santa Cruz Biotechnology, Inc. (Santa Cruz, CA). The monoclonal antiphosphotyrosine PY20 antibody was purchased from Transduction Laboratories (Lexington, KY). The Super signal kit was from Pierce. Trizol, fetal bovine serum, horse serum, and all reagents for cell cultures were from Life Technologies, Inc. The protein kinases inhibitors *N*-[2-(*p*-bromocinnamylamino)ethyl]-5-isoquinolinesulfonamide (H89) and KT5720 were purchased from Biomol (Plymouth Meeting, PA). 8-(4-chlorophenyl-thio)-adenosine 3′,5′-cyclic monophosphate sodium salt (8-CPT), chelerythrine chloride, bisindoleylmaleimide I, phorbol 12-myristate 13-acetate (PMA), 1,2-bis-(o-aminophenoxy)ethane-*N*,*N*,*N*′,*N*′-tetraacetic acid tetra-(acetoxymethyl)-ester (BAPTA-AM), 1-[2-(5-carboxyoxazol-2-

FSK **DA**
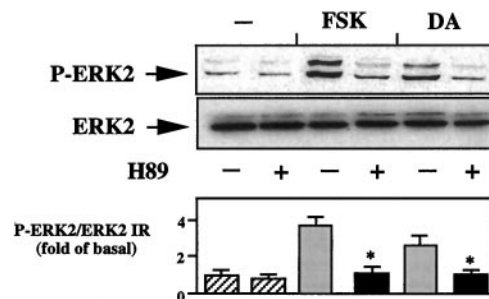

FIG. 2. **Forskolin- and dopamine-induced ERK2 phosphorylation is mediated by PKA.** *A*, cells were preincubated with the PKA inhibitor H89 (20 μM) for 30 min and then left untreated (−) or stimulated (+) for 10 min with forskolin (*FSK*, 20 μM) or with dopamine (*DA*, 100 μM). Total cell lysate extracts were then analyzed by Western blot with antibodies against dually phosphorylated (Thr^{202} and Tyr^{204}) ERKs (*P-ERK2*, *upper panel*) or against phosphorylation state-independent ERKs (*ERK2*, *lower panel*), to normalize for the total amount of ERKs. Data are reported as dually phosphorylated/phosphorylation state-independent ERK immunoreactivity (*IR*), and the average -fold increase (mean ± S.E.) over basal level is reported in the *bar graph* (*n* = 4). *, $p < 0.05$ compared with the correspondent stimulus without inhibitor.

yl)-6-aminobenzo-furan-5-oxy]-2-(2′-amino-5′methylphenoxy)-ethane *N*,*N*,*N*′,*N*′-tetraacetic acid pentacetoxymethyl ester (fura-2/AM), A23187, 2′-amino-3′-methylflavone (PD98059), EGTA, [12-(2-cyano-ethyl)-6,7,12,13-tetrahydro-13-methyl-5-oxo-5H-indolo[2,3-a]pyrrolo[3, 4-c]carbazole] (Gö6976), and thapsigargin were from Alexis Corp. (San Diego, CA). Dopamine, sulpiride, SCH 23390, SKF-38393, D-(−)-2-amino-5-phosphonopentanoic acid (APV), and (+)-MK-801 hydrogen maleate (dizolcipine) were from RBI (Natick, MA). GST-Sepharose beads and Hybond nylon membranes were from Amersham Pharmacia Biotech. The bacterial lysate containing the GST fusion protein of the minimal Rap1-binding domain of ralGDS (GST-ral-RBD) was a generous gift of Dr. M. Freissmuth (Institute of Pharmacology, University of Vienna, Austria). *N*-Acetyl myelin basic protein 4–14 was from Roche Molecular Biochemicals. [γ-^{32}P]ATP was from PerkinElmer Life Sciences. All the other reagents were purchased from Sigma.

Cell Culture—Primary cultures were obtained as previously described (18). Briefly, striata of 16–17-day-old Harlan Sprague-Dawley rat embryos were dissected and incubated with papain. Tissue fragments were mechanically dissociated, and the cells were plated in 60-mm diameter poly-L-lysine-coated (10 μg/ml) dishes and grown in 1:1 minimal essential medium/F-12 medium containing 2 mM glutamine, 2.5% fetal bovine serum, and 2.5% horse serum. About 48 h after plating, 10 μM cytosine-C arabinoside was added to the cultures to prevent the growth of nonneuronal cells. The cells were grown for 6 days *in vitro* for intracellular Ca^{2+} measurement experiments (see below) or 12 days *in vitro* for all other experiments. The total percentage of glial cells was below 5%, as assessed by glial fibrillary acid protein staining and counterstaining with 1% cresyl violet. Unless otherwise indicated, cells were rinsed twice with Krebs buffer and then left for 20 min in Krebs buffer before stimulation with the indicated agents.

In the experiments with BAPTA-AM, the cells were preincubated for the indicated time with BAPTA-AM and then incubated with stimulating agents in Krebs buffer. Experiments in which the role of excitatory amino acids was studied were performed in the presence of 1 μM tetrodoxin to block action potentials and excitatory amino acid release.

Intracellular Ca^{2+} Measurement—The intracellular Ca^{2+} concentration was measured with the fluorescent Ca^{2+} indicator fura-2/AM. Striatal cells, prepared as described above, were plated at low density into 24-well multiwell plates containing 13-mm glass coverslips previously coated with 10 μg/ml poly-L-lysine. After 6 days *in vitro*, cells were washed twice with Krebs buffer and then incubated in the same buffer containing 5 μM fura-2/AM at 37 °C in a humidified incubator with 5% CO$_2$ for 30 min, followed by a postincubation period in the same buffer for 30 min. The dye-loaded cells were epi-illuminated with light from a 75-watt xenon lamp filtered through 340- and 380-nm interference filters, and the fluorescence emitted at 510 nm was revealed by a photon-counting photomultiplier. The 340/380-nm fluorescence ratio, averaged over a period of 2 s, was measured for 10 min in the Krebs buffer, and this value was taken as basal reference value. The stimulating agents were added as 10× concentrated solution, and then changes in the 340/380-nm ratio were monitored for the time indicated

in Fig. 9. For each experimental condition, fluorescence responses were taken in at least three fields on each coverslip.

Pull-down Assay for the Determination of Rap1 Activation—The pull-down assay for the determination of Rap1 activation was carried out as previously reported (19). Briefly, the GST fusion protein of the minimal Rap1-binding domain of ralGDS (ral-RBD) was induced in *Escherichia coli* (strain BL21DE3) by isopropyl-1-thio-β-D-galactopyranoside, and bacterial lysates were prepared as described (19). The GST fusion protein was immobilized by incubating the bacterial lysate for 1 h at 4 °C with glutathione-Sepharose preequilibrated in pull-down buffer (50 mM Tris buffer, pH 7.5, 200 mM NaCl, 2 mM MgCl$_2$, 1 mM phenyl-methylsulfonyl fluoride, 10% glycerol, 1% Nonidet P-40, 2 μg/ml apro-tinin, 1 μg/ml leupeptin). Sepharose beads were washed three times to remove excess GST fusion protein. After stimulation with agonists for 10 min, the cells were rinsed twice with stimulation buffer and then chilled immediately in pull-down buffer, and then cell lysate was cleared by centrifugation at 10,000 $\times$ g for 10 min at 4 °C. Approximately 5% of the total cell lysate was analyzed to normalize for the total amount of Rap1. The remaining supernatant (about 500 μg of proteins) was incubated with the GST-Sepharose beads (50 μl of a 1:1 slurry containing about 10 μg of immobilized GST fusion protein) for 2 h to allow for the association of activated Rap1 with the effector-GST fusion protein. Samples were washed twice with pull-down buffer, resuspended in Laemmli sample buffer and applied to SDS-polyacrylamide gels. The Rap1 band was then visualized using specific antibodies in a 1:1000 dilution by immunoblot analysis (see below).

Immunoblot Analysis—Stimulated cells were rinsed twice with ice-cold phosphate-buffered saline and then lysed in 400 μl of ice-cold lysis buffer (10 mM Tris-HCl, pH 7.5, 140 mM NaCl, 1% Nonidet P-40, 1 mM orthovanadate, 1 mM phenylmethylsulfonyl fluoride, 2 μg/ml aprotinin, 2 μg/ml pepstatin, and 2 μg/ml leupeptin). Cell lysate were centrifuged at 16,000 $\times$ g for 5 min at 4 °C, and the supernatant was incubated for 15 h at 4 °C with primary antibodies and then with 15 μl of protein A-agarose for 1 h. Immunoprecipitates were washed three times with lysis buffer and resuspended either in SDS-sample buffer for immuno-blot experiments or in kinase buffer for immunocomplex protein kinase assay (see below). Western blot analysis was carried out either on 20 μg of nuclear extracts (for phosphorylated CREB, phosphorylation state-independent CREB, and p90^{RSK}), 20 μg of total cell lysate (for phospho-rylated ERK and phosphorylation state-independent ERK), or immuno-precipitates for PYK2. Proteins resolved by 12.5% (PCREB, CREB, ERK, and PERK) or 7% (PYK2 and p90^{RSK}) SDS-polyacrylamide gel electrophoresis were transferred to nitrocellulose membranes by tank blotting overnight at 4 °C. The membranes were rinsed in Tris-buffered saline (TBS) (composition 10 mM Tris-HCl, pH 8.0, 150 mM NaCl, and 0.05% Tween 20), incubated for 1 h in TBS containing 4% nonfat dry milk (TBSM), and then incubated overnight at 4 °C with primary an-tibodies in TBSM. After three 15-min washes in TBS, the membranes were incubated in TBSM for 1 h at room temperature with horseradish peroxidase-conjugated goat polyclonal anti-rabbit IgG for rabbit poly-clonal primary antibodies, or with horseradish peroxidase-conjugated goat polyclonal anti-mouse IgG for mouse monoclonal primary antibod-ies. The chemiluminescent signals were detected using the Super signal kit, and the films were scanned using an Agfa T1200 scanner with Photolook software. The band intensity was quantified with NIH Image software. The same protocol was used for the detection of tyrosine-phosphorylated PYK2 using the mouse monoclonal antibody specific to phosphotyrosine PY20, except that 1% bovine serum albumin was used instead of 4% nonfat dry milk.

Protein Kinase Assay—Cells were preincubated with protein kinase inhibitors as reported in the figure legends and then stimulated with the indicated agents. *In vitro* PKA and PKC activities were performed as previously reported (18, 20).

Northern Blot Analysis—Striatal cultures were treated with appro-priate stimuli for the indicated time and rinsed twice with phosphate-buffered saline. The RNA extraction reagent Trizol was added directly to each culture dish. Total RNA was extracted with a 1:10 volume of chloroform, and the upper aqueous phase was precipitated overnight at −20 °C with a 1:1 volume of isopropyl alcohol. Total RNA was pelleted by centrifugation at 20,000 $\times$ g for 15 min at 4 °C, washed twice with ethanol, and quantified by UV spectrophotometry at 260 nm. Total RNA (10 μg) was size-resolved on a 1.1% denaturing agarose gel con-taining 1 M paraformaldehyde in 20 mM MOPS, pH 7.0, 5 mM sodium acetate, 1 mM EDTA and capillary-blotted overnight in 10$\times$ SSC onto a positively charged Hybond nylon membrane. The membranes were UV-autocross-linked and then prehybridized for 1 h at 65 °C in 0.5 M sodium-phosphate buffer, pH 7.3, 7% SDS, 1 mM EDTA. Hybridization was carried out for 16 h at 65 °C in 50 ml of prehybridization solution
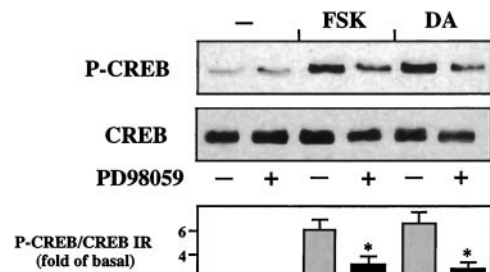

FIG. 3. **Forskolin- and dopamine-induced CREB phosphoryla-tion is mediated by MEK.** Cells were preincubated for 30 min with the MEK inhibitor PD98059 (50 μM) and then left untreated (−) or stimulated (+) for 10 min with forskolin (*FSK*, 20 μM) or with dopamine (*DA*, 100 μM). CREB phosphorylation in nuclear extracts was analyzed as described in the legend of Fig. 1. Data are reported as P-CREB/CREB immunoreactivity (*IR*), and the average -fold increase (mean $\pm$ S.E.) over basal level is reported in the *bar graph* ($n = 4$). *, $p < 0.05$ compared with the correspondent stimulus without inhibitor.

to which about 1×10^6 cpm/ml of a full-length cDNA c-*fos* or 18 S ribosomal gene (internal loading control) cDNA random primed ^{32}P-labeled probes were added. Membranes were washed three times for 2 min in 300 ml of prewarmed (65 °C) washing solution (50 mM Na$_2$HPO$_4$-NaH$_2$PO$_4$, pH 7.4, 1% SDS) and once in 100 ml of the same solution on a shaking platform for 30 min at 65 °C. The radioactivity associated with the membranes was visualized and quantified with a Cyclone storage phosphor system (Packard Instrument Co.).

Statistical Analysis—Results are expressed as mean $\pm$ S.E., and the significance of differences among treatments was evaluated using Stu-dent's t test for paired data or analysis of variance by Dunnett's test.

RESULTS

Activation of the cAMP/PKA Pathway Induces CREB Phos-phorylation in Striatal Neurons—The striatum is the brain area with the most abundant dopaminergic innervation, and striatal neurons in primary cultures express all of the dopa-minergic receptor subtypes. We first sought to determine which receptor subtypes and signal transduction pathways are in-volved in CREB phosphorylation induced by the neurotrans-mitter dopamine in cultured striatal neurons. Dopaminergic regulation of Ser^{133} CREB phosphorylation was investigated by using selective agonists and antagonists specific for the D$_1$-like and D$_2$-like dopaminergic receptor subtypes. Dopa-mine-induced increase in Ser^{133} CREB phosphorylation (2.1 $\pm$ 0.2-fold basal level, $n = 4$) was mimicked by the D$_1$-like recep-tor agonist SKF38393, not affected by the D$_2$-like receptor antagonist sulpiride, and blocked by the D$_1$-like antagonist SCH 23390 (Fig. 1*A*). To confirm the involvement of cAMP and to rule out any possible G protein-dependent activation of cAMP-independent signal transduction pathways, CREB phos-phorylation was stimulated by agents capable of increasing cAMP formation downstream of dopamine receptors. The mem-brane-permeable cAMP analogue 8-CPT (200 μM) and the di-rect activator of adenylylcyclase forskolin (20 μM) induced a significant increase (3.2 $\pm$ 0.5-fold basal level, $n = 4$) of CREB phosphorylation, similar to that induced by 100 μM dopamine.

The recent characterization of a family of cAMP-binding proteins that directly activates the Ras-like Rap1 protein (21), raises the possibility that the forskolin-induced CREB phos-phorylation might be mediated by a cAMP-dependent but PKA-independent mechanism; this mechanism seems unlikely under our conditions, since forskolin-induced CREB phospho-rylation was blocked by the PKA inhibitors KT5720 and H89 (Fig. 1*B*).

PKA-induced ERK Activation and CREB Phosphorylation Require PKC Activity—In different experimental models (16, 22), the activation of the cAMP/PKA-dependent pathway leads to activation of the ERK pathway. To assess whether this
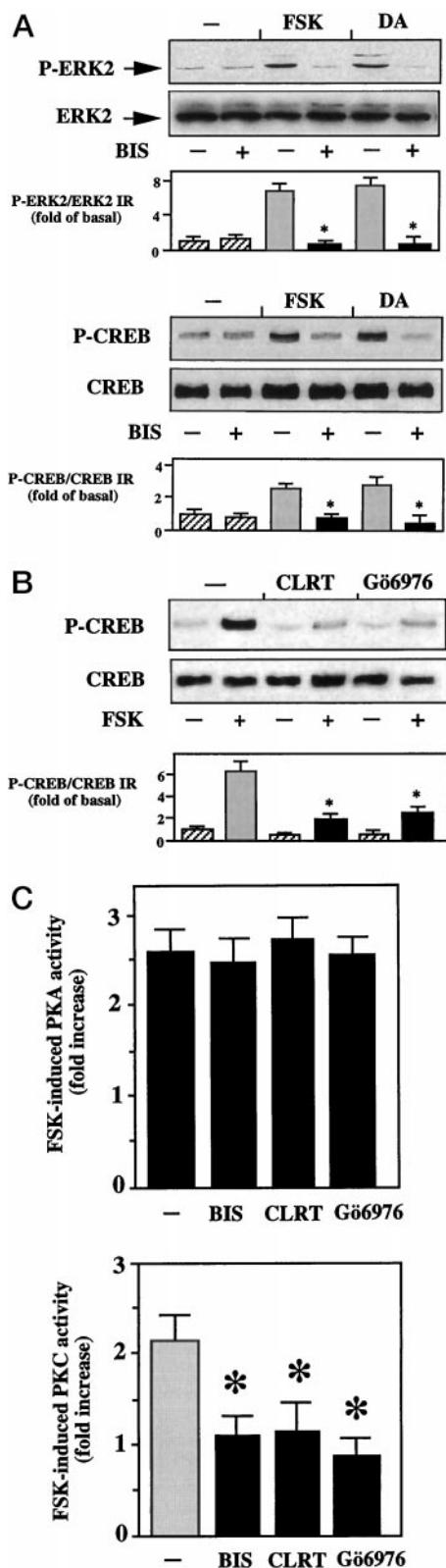
FIG. 4. **Forskolin- and dopamine-induced CREB phosphorylation is blocked by PKC inhibitors.** *A*, cells were preincubated for 30 min with the PKC inhibitor bisindoleylmaleimide I (*BIS*, 10 μM) and then left untreated (−) or stimulated (+) for 10 min with forskolin (*FSK*, 20 μM) or with dopamine (*DA*, 100 μM). P-CREB and P-ERK2 phosphorylation was analyzed as described in the legends of Figs. 1 and 2, respectively. Data are reported as P-ERK2/ERK2 immunoreactivity (*IR*) or P-CREB/CREB immunoreactivity (*IR*), and the average -fold increase (mean ± S.E.) over basal level is reported in the *bar graph* (*n* = 4). *, *p* < 0.05 compared with the correspondent stimulus without inhibitor. *B*, cells were preincubated for 30 min with the PKC inhibitors chelerythrine chloride (*CLRT*, 1 μM) or Gö6976 (5 μM) and then left

cross-talk occurs in cultured striatal neurons, we performed a set of experiments using a phosphospecific antibody directed against the dually phosphorylated ERK isoforms ERK1 and ERK2. We found that DA and forskolin stimulated predominantly the phosphorylation of the ERK p42 isoform ERK2 (FSK: 4.5 ± 0.8-fold over basal level, *n* = 4; DA: 3.2 ± 0.5-fold over basal level, *n* = 4), and this effect was PKA-dependent, being reduced by the PKA inhibitor H89 (Fig. 2). PKA-induced activation of the ERK pathway was an intermediate step in PKA-induced CREB phosphorylation, since the ERK kinase (MEK) inhibitor PD98059 strongly blocked CREB phosphorylation induced by forskolin and dopamine (Fig. 3). In previous *in vitro* kinase assays, we found that, under our experimental conditions, the effect of PD98059 was specific for the ERK pathway and did not interfere with the activity of other kinases such as PKA and CaMKs (data not shown).

Since in the hippocampus the ERK pathway could be activated by PKC (22), we investigated the role of this kinase in cAMP/PKA-induced CREB phosphorylation. The PKC inhibitor bisindoleylmaleimide I strongly reduced DA- and FSK-induced ERK2 and CREB phosphorylation (Fig. 4*A*); the same results were obtained using two other specific PKC inhibitors, chelerythrine chloride and Gö6976 (Fig. 4*B*). *In vitro* kinase assays demonstrated that, under our experimental conditions, PKC inhibitors blocked PKC activity but did not interfere with nuclear PKA activity (Fig. 4*C*). To further confirm a causal relationship between PKC activation and ERK2/CREB phosphorylation, we investigated the functional consequence of short and long term treatment of striatal cells with the direct PKC activator PMA on ERK and CREB phosphorylation. When cells were stimulated for 10 min with 1 μM PMA to activate PKC, the MEK inhibitor PD98059 blocked both PMA-induced ERK2 and CREB phosphorylation (Fig. 5*A*). Accordingly, when cells were treated for 18 h with 10 nM PMA to desensitize PKC, forskolin-induced ERK2 and CREB phosphorylation were significantly reduced, as compared with untreated cells (Fig. 5*B*). Taken together, these experiments strongly suggest that PKA causes CREB phosphorylation via a PKC/ERK-dependent pathway.

PKA-induced CREB Phosphorylation and CRE-dependent Gene Transcription Require Intracellular Ca²⁺—Previous studies have shown that neuronal Ca²⁺ represents a link between the ERK- and PKA-dependent pathways (16). These observations prompted us to investigate the Ca²⁺ requirement in PKA-induced CREB phosphorylation mediated by ERK in striatal neurons; a set of experiments was performed using the cell-permeable intracellular Ca²⁺ chelator BAPTA-AM. When neurons were preincubated with BAPTA-AM (50 μM) for 30 min, both ERK2 (Fig. 6*A*) and CREB phosphorylation (Fig. 6*B*) induced by forskolin were significantly reduced.

Having established the requirement of Ca²⁺ in PKA-mediated CREB phosphorylation, we then analyzed the possible

untreated (−) or stimulated (+) for 10 min with forskolin (*FSK*, 20 μM). CREB phosphorylation in nuclear extracts was analyzed as described in the legend to Fig. 1. Data are reported as P-CREB/CREB immunoreactivity (*IR*), and the average -fold increase (mean ± S.E.) over basal level is reported in the bar graph (*n* = 4). *, *p* < 0.05 compared with the correspondent stimulus without inhibitor. *C*, cells were preincubated for 30 min with the PKC inhibitor bisindoleylmaleimide I (*BIS*, 10 μM), chelerythrine chloride (*CLRT*, 1 μM), or Gö6976 (5 μM) and then left untreated (−) or stimulated (+) for 10 min with forskolin (*FSK*, 20 μM). Cells were harvested, and PKA and PKC *in vitro* activities were assayed as reported in the references cited under "Experimental Procedures." Data are reported as forskolin-induced kinase activity increase normalized to the corresponding basal level in the presence of the indicated inhibitor. The average -fold increase (mean ± S.E.) is reported in the *bar graph* (*n* = 4). *, *p* < 0.05 compared with forskolin without inhibitor.
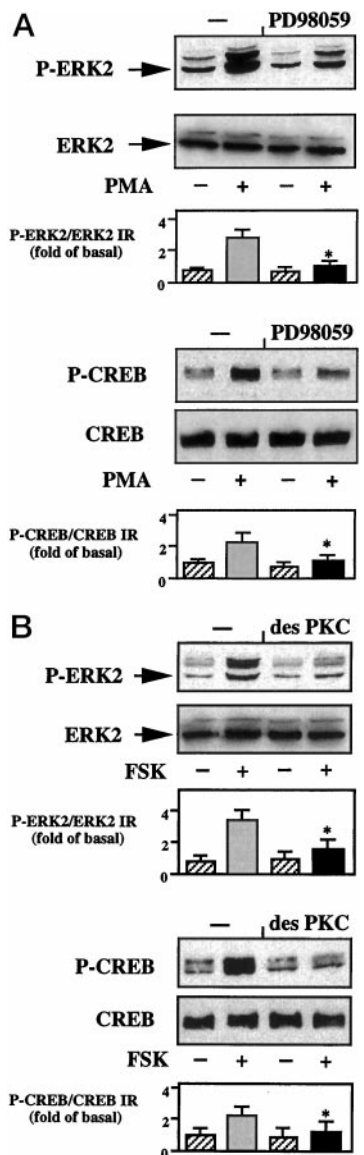
FIG. 5. **Activation of PKC induces ERK2 and CREB phosphorylation.** *A*, cells were preincubated for 30 min with the MEK inhibitor PD98059 (50 μM) and then left untreated ($-$) or stimulated ($+$) for 10 min with PMA (1 μM). P-CREB and P-ERK2 phosphorylation was analyzed as described in the legends of Figs. 1 and 2, respectively. Data are reported as P-ERK2/ERK2 or P-CREB/CREB immunoreactivity (*IR*), and the average -fold increase (mean $\pm$ S.E.) over basal is reported in the bar graph ($n = 4$). *, $p < 0.05$ compared with the correspondent stimulus without inhibitor. *B*, cells were left untreated ($-$) or pretreated for 18 h with 10 nM PMA (*des PKC*) to desensitize PKC. Then cells were left untreated ($-$) or stimulated ($+$) for 10 min with forskolin (*FSK*, 20 μM). P-CREB and P-ERK2 phosphorylation was analyzed as described in the legends of Figs. 1 and 2, respectively. Data are reported as P-ERK2/ERK2 or P-CREB/CREB immunoreactivity (*IR*), and the average -fold increase (mean $\pm$ S.E.) over basal level is reported in the *bar graph* ($n = 4$). *, $p < 0.05$ compared with forskolin in PMA-untreated cells.

involvement of L-type Ca^{2+} channels and NMDA receptors in this mechanism. Both L-type Ca^{2+} channels and NMDA receptors have been previously shown to be involved in CREB phosphorylation and CRE-dependent gene expression (7). Preincubation of striatal cells with the competitive NMDA antagonist APV or the noncompetitive NMDA antagonist MK-801 did not interfere with forskolin-induced CREB phosphorylation (Fig. 7*A*). This finding clearly demonstrates that in striatal neurons NMDA receptors are not responsible for the intracellular Ca^{2+} elevation required in forskolin-induced CREB phosphorylation.
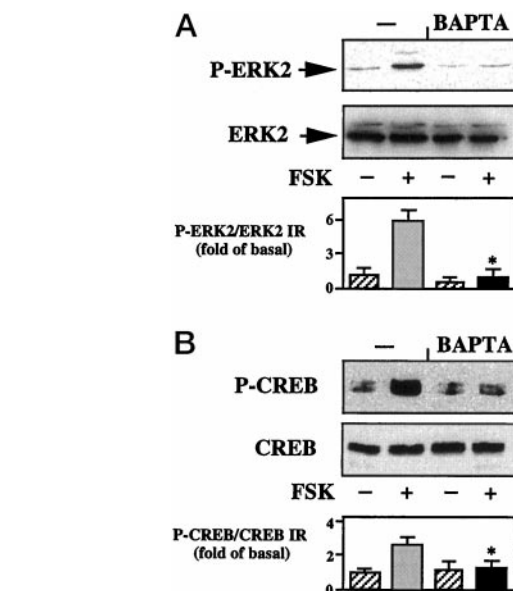

FIG. 6. **Forskolin-induced ERK2 and CREB phosphorylation requires intracellular Ca^{2+}.** Cells were preincubated for 30 min with BAPTA-AM (50 μM) and then left untreated ($-$) or stimulated ($+$) for 10 min with forskolin (*FSK*, 20 μM). P-CREB and P-ERK2 phosphorylation was analyzed as described in the legends of Figs. 1 and 2, respectively. Data are reported as P-ERK2/ERK2 or P-CREB/CREB immunoreactivity (*IR*), and the average -fold increase (mean $\pm$ S.E.) over basal level is reported in the *bar graph* ($n = 4$). *, $p < 0.05$ compared with forskolin in BAPTA-untreated cells.

In a subset of striatal neurons, PKA-induced phosphorylation of the L-type voltage-sensitive Ca^{2+} channel increases the peak current through these channels, thereby augmenting the amount of Ca^{2+} entering the cell (23). We therefore investigated whether extracellular Ca^{2+} was required for PKA-induced CREB phosphorylation in striatal neurons. To our surprise, we found that neither the extracellular Ca^{2+} chelator EGTA nor the specific L-type voltage-dependent Ca^{2+} channel blocker nifedipine interfered with CREB phosphorylation induced by forskolin (Fig. 7*B*). To test whether an increase in intracellular Ca^{2+} could induce CREB phosphorylation, we analyzed the effect of the SERCA pump inhibitor thapsigargin. As expected from the previous experiments, thapsigargin induced an increase (2.8 ± 0.3-fold basal level, $n = 4$) of CREB phosphorylation (Fig. 7*B*). Interestingly, we found that neither nifedipine nor MK-801 interfered with forskolin-induced ERK2 phosphorylation (Fig. 7*C*), strongly suggesting, although without proving definitively, that ERK2 activation mediates PKA-dependent CREB phosphorylation.

To investigate whether intracellular Ca^{2+} was also required for the cAMP/PKA-induced gene transcription, we measured the mRNA levels of the immediate early gene c-*fos*, which contains in its promoter a CRE sequence. Treatment of striatal neurons for 30 min with 20 μM forskolin induced a 2.3 ± 0.3-fold increase ($n = 4$) of c-*fos* mRNA over basal levels; when striatal neurons were preincubated for 30 min with BAPTA-AM (50 μM) to chelate intracellular Ca^{2+} or with the MEK inhibitor PD98059 to block the ERK pathway, forskolin-induced increase of *c-fos* mRNA was prevented (Fig. 8).

PKA Activation Releases Intracellular Ca^{2+}—Our experiments with BAPTA-AM and thapsigargin indicate that PKA activation might induce the release of intracellular Ca^{2+} from Ca^{2+} store organelles in striatal neurons. To test this hypothesis, intracellular Ca^{2+} measurements in striatal neurons were performed using the fluorescent Ca^{2+} probe fura-2/AM. The Ca^{2+} ionophore A23187 (5 μM), which causes a large Ca^{2+} entry, was first tested as a positive control (Fig. 9, *open*

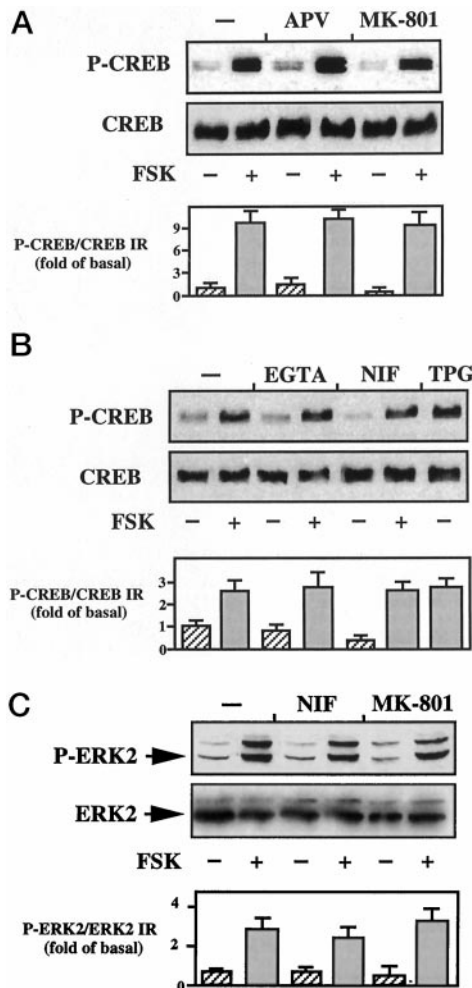*Intracellular Calcium Induces CREB Phosphorylation*

FIG. 7. **Forskolin-induced CREB and ERK2 phosphorylation is not mediated by Ca²⁺ channels or NMDA receptors.** *A*, cells were preincubated for 15 min with the competitive NMDA receptor antagonist APV (100 μM) or with the noncompetitive NMDA receptor antagonist MK-801 (10 μM) and then left untreated (−) or stimulated (+) for 10 min with forskolin (*FSK*, 20 μM). P-CREB phosphorylation was analyzed as described in the legend to Fig. 1. Data are reported as P-CREB/CREB immunoreactivity (*IR*), and the average -fold increase (mean ± S.E.) over basal level is reported in the *bar graph* ($n = 4$). *B*, cells were preincubated for 15 min with the extracellular Ca²⁺ chelator EGTA (5 mM) and the voltage-sensitive Ca²⁺ channel blocker nifedipine (*NIF*, 10 μM) and then left untreated (−) or stimulated (+) for 10 min with forskolin (*FSK*, 20 μM) or with the SERCA pump inhibitor thapsigargin (*TPG*, 200 nM). P-CREB phosphorylation was analyzed as described in the legend of Fig. 1. Data are reported as P-CREB/CREB immunoreactivity (*IR*), and the average -fold increase (mean ± S.E.) over basal level is reported in the *bar graph* ($n = 4$). *C*, cells were preincubated for 15 min with the voltage-sensitive Ca²⁺ channel blocker nifedipine (*NIF*, 10 μM) or with noncompetitive NMDA receptor antagonist MK-801 (10 μM) and then left untreated (−) or stimulated (+) for 10 min with forskolin (*FSK*, 20 μM). P-ERK2 phosphorylation was analyzed as described in the legend to Fig. 2. Data are reported as P-ERK2/ERK2 immunoreactivity (*IR*), and the average fold increase (mean ± S.E.) over basal level is reported in the bar graph ($n = 4$).
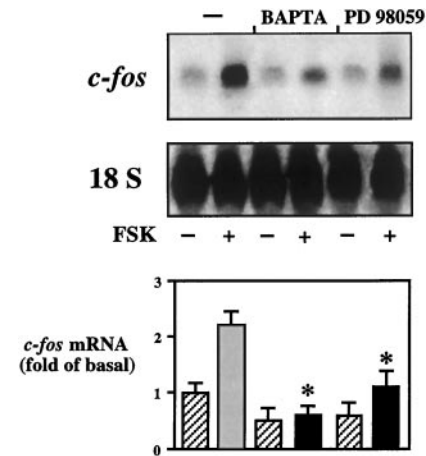

FIG. 8. **Forskolin-induced c-*fos* transcription is mediated by Ca²⁺ and ERK signaling pathways.** Cells were preincubated for 30 min with the intracellular Ca²⁺ chelator BAPTA-AM (50 μM) or with the MEK inhibitor PD98059 (50 μM) and then left untreated (−) or stimulated (+) with forskolin (*FSK*, 20 μM) for 30 min. Total RNA was extracted from the cell lysates, separated by 1% gel agarose electrophoresis, and blotted to nylon membranes. The membrane was hybridized with a c-*fos* (*upper panel*) and an 18 S ribosomal RNA (18 S, *lower panel*) probe and then exposed to x-ray film for autoradiography. Data are reported as c-*fos* mRNA levels normalized to 18 S mRNA, and the average -fold increase (mean ± S.E.) over basal level is reported in the *bar graph* ($n = 4$). *, $p < 0.05$ compared with forskolin without inhibitor.

skolin still elicited a significant sharp, very short lasting (about 7 s) and fast decreasing rise in intracellular Ca²⁺ levels (Fig. 9, *open circles*). Taken together, these data indicate that, in addition to playing a role in regulating voltage-dependent Ca²⁺ channel function, PKA may also increase intracellular Ca²⁺ by releasing Ca²⁺ from intracellular stores.

PKA Stimulation Induces Rap1 and PYK2 Activation—In several experimental models, the family of small G proteins plays a key role in Ca²⁺-induced activation of ERK. Recently, it has been reported that Rap1, a Ras-like small G protein that may activate the ERK pathway by interacting with the kinase B-Raf, is activated by membrane depolarization in a PKA-dependent manner (16) and by PKA via the ERK pathway (24). To test the possibility that Rap1 participates in the signaling pathway responsible for PKA-induced CREB phosphorylation, we decided to investigate the activation of Rap1 by means of a pull-down assay using the GST-ralRBD fusion protein. Stimulation of striatal cells with 20 μM forskolin for 10 min induced a large increase in the amount of Rap1-GTP (Fig. 10*A*). We then investigated the effects of both kinase inhibitors and of agents capable of interfering with intracellular Ca²⁺ levels. Forskolin-induced Rap1 activation was blocked by the PKA inhibitor H89, but not by the specific PKC inhibitor bisindoleylmaleimide I. Intracellular Ca²⁺ release appears to be necessary and sufficient for Rap1 activation, because Rap1 activation was not observed in the presence of BAPTA-AM and was mimicked by elevation of intracellular Ca²⁺ induced by thapsigargin (Fig. 10*A*). These data indicate that forskolin mainly stimulates Rap1 activation in a PKA/Ca²⁺-dependent but PKC-independent manner, suggesting that the role of PKC in PKA-dependent CREB phosphorylation is likely to be downstream of Rap1.

Finally, since in the central nervous system the concomitant elevation of intracellular Ca²⁺ and activation of PKC leads to tyrosine phosphorylation and activation of PYK2 (25), we investigated whether PYK2 was activated by PKA under our experimental conditions. As expected, PKA activation induced an increase of tyrosine phosphorylation of PYK2 immunoprecipitated from total cell lysate of striatal neurons (Fig. 10*B*).
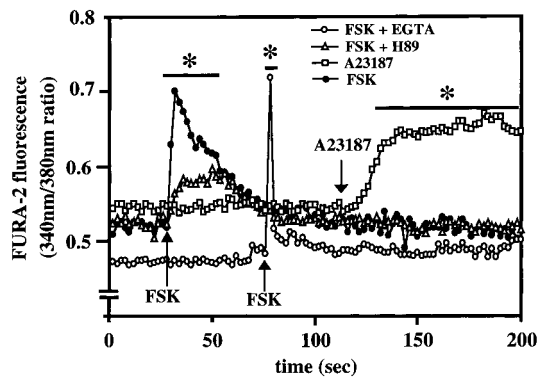
squares, $n = 4$). Application of forskolin (20 μM) to fura-2/AM-loaded neurons caused a significant long lasting (about 30 s) and slowly decreasing rise in intracellular Ca²⁺ levels (Fig. 9, *full circles*, $n = 4$). The amplitude, but not the shape, of the forskolin-induced Ca²⁺ response was greatly reduced by preincubating the cells with the PKA inhibitor H89 (20 μM; Fig. 9, *open triangles*, $n = 4$). Finally, to study the role of extracellular Ca²⁺, fura-2/AM-loaded neurons were preincubated with the chelator of extracellular Ca²⁺ EGTA (5 mM) and then stimulated with forskolin. In the absence of extracellular Ca²⁺, for-

FIG. 9. **Forskolin induces intracellular Ca²⁺ release.** Fura-2/AM-loaded striatal neurons were preincubated for 30 min with EGTA (5 mM) or the PKA inhibitor H89 (10 μM) and then stimulated at 21 °C at the time indicated by the *arrows* with forskolin (*FSK*, 20 μM) or the Ca²⁺ ionophore A23187 (5 μM). Fura-2 fluorescence (340/380-nm ratio) was measured every 2 s, and data were analyzed as described under "Experimental Procedures." The figure shows averages obtained from a total of 15 cells in one representative experiment; the S.E. (not shown) was less than 15%. Within each optic field, the number of cells that responded to the treatment was 5.2 ± 1.4 ($n = 24$ optic fields). A total of four independent experiments (four different sets of cultures) were performed and gave similar results. *, $p < 0.05$ compared with their respective basal (unstimulated) values.

DISCUSSION

This study describes a novel mechanism by which activation of the cAMP/PKA-dependent pathway may stimulate CREB phosphorylation in striatal neurons (Fig. 11). Activation of PKA, induced by dopamine or forskolin, releases Ca²⁺ from the intracellular stores, which in turn activates the Rap1·B-Raf complex whose main target is the phosphorylation of ERK. Finally, the activation of ERK induces CREB phosphorylation, probably via the translocation of the ERK·RSK complex into the nucleus. The prevailing model dictates that an increase of cAMP induces CREB phosphorylation via a mechanism in which the PKA catalytic subunit translocates into the nucleus and directly phosphorylates CREB; in this mechanism, the localization of PKA may contribute to enhance cAMP-dependent CREB phosphorylation and CRE-dependent gene expression (20). However, several recent studies have demonstrated that, in addition to this direct PKA-dependent pathway, other signaling pathways, such as the ERK pathway (10), can induce CREB phosphorylation in a PKA-dependent manner. The participation of the ERK pathway appears to be very important for PKA-dependent transcription, because several neurotransmitter receptor systems (22) as well as depolarization-induced Ca²⁺ influx (16) have been shown to activate the ERK pathway via a PKA-mediated mechanism. This mechanism appears to have an important functional role, since a previous study in *Aplysia* has shown that long term facilitation involves PKA-dependent activation of ERKs (26). In agreement with these data, we have demonstrated that in striatal neurons the novel mechanism involving PKA-induced intracellular Ca²⁺ release participates in ERK and CREB phosphorylation and ultimately regulates the transcription of the immediate early gene c-*fos*.

Previous studies in various experimental models have shown that the functionality of intracellular Ca²⁺ store organelles could be modulated by PKA-dependent phosphorylation *in vivo* and *in vitro*. The neuronal type-I IP3 receptor, immunopurified from rat cerebellar membranes, can be phosphorylated by PKA *in vitro* (27), and activation of PKA induces phosphorylation of the type-I IP3 receptor in cerebellar slices (27) and in cultured cells (28, 29). Notably, a recent paper has described that, in cardiac tissue, PKA-dependent phosphorylation of ryanodine receptor/Ca²⁺ release channel regulates the channel open prob-
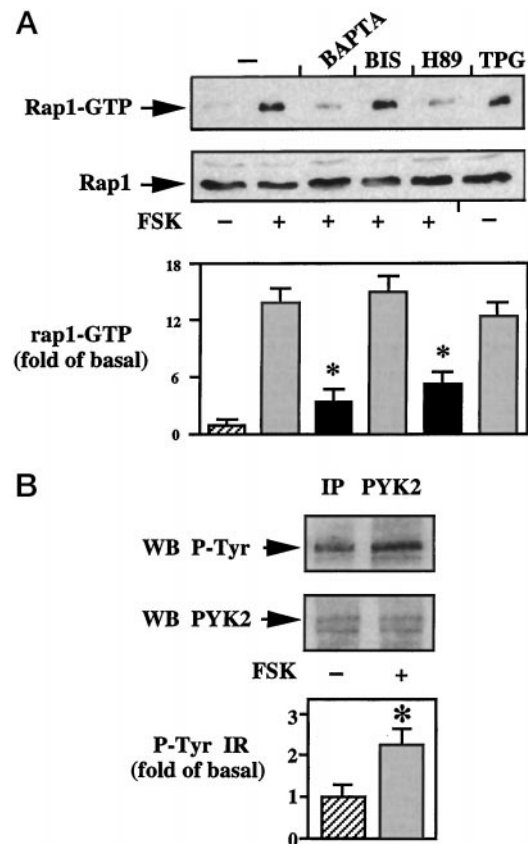

FIG. 10. **Forskolin activates Rap1 and PYK2.** *A*, cells were preincubated for 30 min with BAPTA-AM (*BAPTA*, 50 μM), the PKC inhibitor bisindoleylmaleimide I (*BIS*, 10 μM), and the PKA inhibitor H89 (20 μM) and then left untreated (−) or stimulated (+) for 10 min with forskolin (*FSK*, 20 μM) or thapsigargin (*TPG*, 200 nM). Preincubation with these agents did not modify basal Rap1-GTP levels (not shown). Total cell lysate (0.5 mg) was processed for the pull-down assay of Rap1 using the GST-ral-RBD protein as described under "Experimental Procedures." Western blot analysis was performed on the pulled down Rap1-GTP (*upper panel*) and on total Rap1 (*lower panel*) in a 5% (25-μg) extract of total cell lysate as a loading control (*bottom panel*). Data are reported as Rap1-GTP immunoreactivity, and the average -fold increase (mean ± S.E.) over basal level is reported in the *bar graph* ($n = 4$). *, $p < 0.05$ compared with forskolin. *B*, cells were stimulated for 10 min with forskolin (*FSK*, 20 μM), and then PYK2 was immunoprecipitated from total cell lysate (1 mg). The immunoprecipitate was analyzed by Western blot with antiphosphotyrosine (*WB P-Tyr*, *upper panel*) or anti-PYK2 (*WB PYK2*, *lower panel*) antibodies as described under "Experimental Procedures." Data are reported as Tyr(P) immunoreactivity (*IR*), and the average -fold increase (mean ± S.E.) over basal level is reported in the *bar graph* ($n = 4$). *, $p < 0.05$ compared with basal level.

ability (30). These studies suggest that PKA-dependent phosphorylation could modulate the functionality of intracellular Ca²⁺ store organelles by increasing their sensitivity to physiological agonists or toward external Ca²⁺. Given the importance of the cross-talk between PKA- and Ca²⁺-dependent pathways, the precise mechanism of PKA-mediated intracellular Ca²⁺ release will certainly become a focus of future studies in neuronal cell physiology.

In PC12 cells and primary cortical neurons, ERK activation induced by Ca²⁺ entry through voltage-sensitive channels or by the release of Ca²⁺ from intracellular stores is mediated by the small G protein Ras (14). Several factors, such as the route and magnitude of Ca²⁺ influx or the subcellular compartmentalization of protein kinases in the cell type under investigation, contribute to determine which signaling pathway upstream of ERK is activated. Several recent studies performed in various cell types have demonstrated that Ca²⁺, in addition to Ras, may also activate ERK via another route involving the Ras
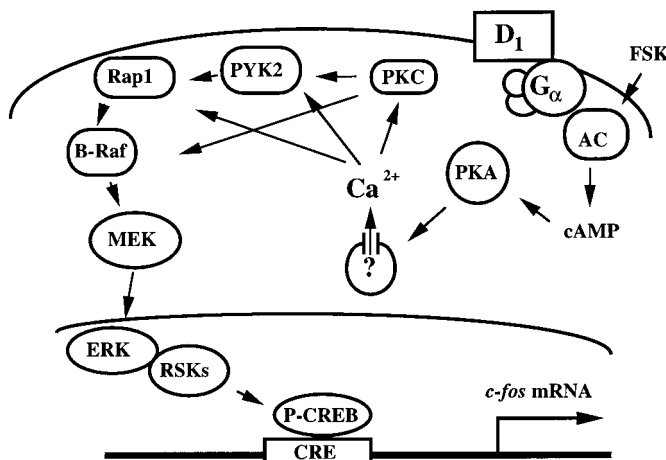
FIG. 11. **Model of PKA-induced CREB phosphorylation mediated by the PKC/ERK-dependent pathway.** Activation of the PKA pathway by stimulation of D_1-like dopamine receptors or by direct activation of adenylylcyclase (*AC*) by forskolin (*FSK*) causes the release of calcium from intracellular stores. Calcium then activates the ERK signaling pathway via a mechanism that could be mediated by PKC, PYK2, and the Rap1·B-Raf complex. Activated ERK translocates into the nucleus and induces CREB phosphorylation and CRE-dependent gene expression (in this case an increase of *c-fos* mRNA) probably via an indirect mechanism involving the family of RSKs.

homologue Rap1 and its effector Raf-like kinase B-Raf. The Rap1·B-Raf system participates in PKA-mediated ERK activation induced by growth factors in PC12 cells (14, 31, 32) and by β_2 adrenergic receptor stimulation in HEK 293 cells (24). In agreement with these reports, we propose that in striatal neurons the Rap1·B-Raf system is an intermediate step in the activation of the ERK pathway triggered by PKA-induced intracellular Ca^{2+} release. This model is in contrast with what was found by other authors in PC12 cells (16), in which depolarization-induced Ca^{2+} entry activates the ERK pathway via a two-step mechanism involving first PKA and then Rap1. In a previous study (33) and in experiments not reported here, we found that, in cultured striatal neurons, Ca^{2+} entry induced by a Ca^{2+} ionophore or by depolarization inhibits cAMP formation, probably interacting with the Ca^{2+}-inhibitable type V adenylyl cyclase isoform, which is abundantly expressed in these neurons (18).

The complexity of Rap1 activation mechanisms in neuronal cells has been emphasized by the characterization of new families of Rap guanine nucleotide exchange factors activated by Ca^{2+} and diacylglycerol (34) or by cAMP and Ca^{2+} (17, 21). On the other hand, our findings demonstrate that, in agreement with another report (35), Rap1 activation is induced by PKA-dependent release of intracellular Ca^{2+} (35). The differences in the mechanism of Rap1 activation are probably due to the differential expression of adenylyl cyclase isoforms and small G protein guanine nucleotide exchange factors in the cell types under investigation. Moreover, since Rap1 activation is not triggered by a PKA- or PKC-dependent phosphorylation, two mechanisms may be considered. First, Rap1 could be directly activated by the novel Rap1GEFs, which in turn are directly activated by Ca^{2+}. Second, Rap1 could be activated indirectly via a multiple step mechanism involving the Ca^{2+}-dependent stimulation of PYK2, which then interacts with Rap1GEF C3G (36). In agreement with this latter hypothesis, in the present study we have found that activation of the cAMP/PKA-dependent pathway leads to activation of the tyrosine kinase PYK2 (25). This is consistent with the observation that, in striatal brain slices, stimulation of D_2 receptors induces tyrosine phosphorylation of PYK2 via a phospholipase C-mediated intracellular Ca^{2+} release (37). So far, it is still unclear whether in

striatum activation of PYK2 is implicated in CREB phosphorylation, because D_2-dependent CREB phosphorylation was not blocked by the broad spectrum tyrosine kinase inhibitor genistein (37).

Although the experiments presented in this study show that in striatal neurons PKC inhibitors block PKA-induced CREB phosphorylation, no conclusion can be drawn about the mechanism by which the cAMP/PKA-dependent pathway activates PKC and at what level PKC modulates CREB phosphorylation. Having excluded a direct role of PKC in Rap1 activation in our model, it is reasonable to assume that PKC acts downstream of Rap1 and upstream of B-Raf. This hypothesis is supported by studies showing that PKC may play a facilitator role on the small G protein-dependent ERK pathway activation by enhancing Raf-1 or B-Raf functionality (38).

In conclusion, we have found that intracellular Ca^{2+} release induced by PKA leads to CREB phosphorylation via a PKC- and ERK-dependent mechanism, most likely involving Rap1 activation. Given the complexity of cross-talk between the cAMP/PKA and the ERK pathways, the plethora of signaling pathways converging on ERK, and the wide array of transcription factors activated by these signaling pathways, this and other studies (16, 23) raise fundamental questions concerning the role of Rap1 and the functional effects of its activation at the level of transcription factor activation and CRE-dependent gene expression.

REFERENCES

1. Burt, D. R., Creese, I., and Snyder, S. H. (1977) *Science* **196,** 326–328
2. Nestler, E. J., Hope, B. T., and Widnell, K. L. (1993) *Neuron* **11,** 995–1006
3. Gonzales, G. A., and Montminy, M. R. (1989) *Cell* **59,** 675–680
4. Sheng, M., McFadden, G., and Greenberg, M. E. (1990) *Neuron* **4,** 571–582
5. Bito, H., Deisseroth, K., and Tsien, R. W. (1996) *Cell* **87,** 1203–1214
6. Deisseroth, K., Heist, E. K., and Tsien, R. W. (1998) *Nature* **392,** 198–202
7. Das, S., Grunert, M., Williams, L., and Vincent, S. R. (1997) *Synapse* **25,** 227–233
8. Ginty, D. D., Bonni, A., and Greenberg, M. E. (1994) *Cell* **77,** 713–725
9. Finkbeiner, S., Tavazoie, S. F., Maloratsky, A., Jacobs, K. M., Harris, K. M., and Greenberg, M. E. (1997) *Neuron* **19,** 1031–1047
10. Impey, S., Obrietan, K., Wong, S. T., Poser, S., Yano, S., Wayman, G., Deloulme, J. C., Chan, G., Storm, D. R. (1998) *Neuron* **21,** 869–883
11. Perkinton, M. S., Sihra, T. S., and Williams, R. J. (1999) *J. Neurosci.* **19,** 5861–5874
12. Vanhoutte, P., Barnier, J. V., Guibert, B., Pages, C., Besson, M. J., Hipskind, R. A., and Caboche, J. (1999) *Mol. Cell. Biol.* **19,** 136–146
13. Kornhauser, J. M., and Greenberg, M. (1997) *Neuron* **18,** 839–842
14. Rosen, L. B., Ginty, D. D., Weber, M. J., and Greenberg, M. E. (1994) *Neuron* **12,** 1207–1221
15. Vossler, M. R., Yao, H., York, R. D., Pan, M. G., Rim, C. S., and Stork, P. J. (1997) *Cell* **89,** 73–82
16. Grewal, S. S., Horgan, A. M., York, R. D., Withers, G. S., Banker, G. A., and Stork, P. J. S. (2000) *J. Biol. Chem.* **275,** 3722–3728
17. deRooji, J., Zwartkruis, F. J., Verheijen, M. H., Cool, R. H., Nijman, S. M., Wittinghofer, A., and Bos, J. L. (1998) *Nature* **396,** 474–477
18. Paolillo, M., Montecucco, A., Zanassi, P., and Schinelli, S. (1998) *Eur. J. Neurosci.* **10,** 1937–1945
19. Seidel, M. G., Klinger, M., Freissmuth, M., and Holler, C. (1999) *J. Biol. Chem.* **274,** 25833–25841
20. Paolillo, M., Feliciello, A., Porcellini, A., Garbi, C., Bifulco, M., Schinelli, S., Ventra, C., Stabile, E., Ricciardelli, G., Schettini, G., and Avvedimento, E. V. (1999) *J. Biol. Chem.* **274,** 6546–6552
21. Kawasaki, H., Springett, G. M., Mochizuki, N., Toki, S., Nakaya, M., Matsuda, M., Housman, D. E., and Graybiel, A. M. (1998) *Science* **282,** 2275–2279
22. Roberson, E. D., English, J. D., Adams, J. P., Selcher, J. C., Kondratick, C., and Sweatt, J. D. (1999) *J. Neurosci.* **19,** 4337–4348
23. Surmeier, D. J., Bargas, J., Hemmings, H. C., Nairn, A. C., and Greengard, P. (1995) *Neuron* **14,** 385–397
24. Schmitt, J. M., and Stork, P. J. S. (2000) *J. Biol. Chem.* **275,** 25342–25350
25. Lev, S., Moreno, H., Martinez, R., Canoll, P., Peles, E., Musacchio, J. M., Plowman, G. D., Rudy, B., and Schlessinger, J. (1995) *Nature* **376,** 737–745
26. Martin, K. C., Michael, D., Rose, J. C., Barad, M., Casadio, A., Zhu, H., Kandel, E. R. (1997) *Neuron* **18,** 899–912
27. Haug, L. S., Jensen, V., Hvalby, Ø., Walaas, S. I., and Østvold, A. C. (1999) *J. Biol. Chem.* **274,** 7467–7473
28. Yoshida, A., Ogura, A., Imagawa, T., Shigekawa, M., and Takahashi, M. (1992) *J. Neurosci.* **12,** 1094–1100
29. Wojcikiewicz, R. J. H., and Luo, S. G. (1998) *J. Biol. Chem.* **273,** 5670–5677
30. Marx, S. O., Reiken, S., Hisamatsu, Y., Jayaraman, T., Burkhoff, D., Rosemblit, N., and Marks, A. R. (2000) *Cell* **101,** 365–376
31. York, R. D., Yao, H., Dillon, T., Ellig, C. L., Eckert, S. P., McCleskey, E. W., and Stork, P. J. (1998) *Nature* **392,** 622–626
32. Yao, H., York, R. D., Misra-Press, A., Carr, D. W., and Stork, P. J. (1998)

J. Biol. Chem. **273,** 8240–8247

33. Schinelli, S., Paolillo, M., and Corona, G. L. (1994) *Mol. Brain Res.* **21,** 162–166
34. Kawasaki, H., Springett, G. M., Toki, S., Canales, J. J., Harlan, P., Blumenstiel, J. P., Chen, E. J., Bany, I. A., Mochizuki, N., Ashbacher, A., Matsuda, M., Housman, D. E., and Graybiel, A. M. (1998) *Proc. Natl. Acad. Sci. U. S. A.* **95,** 13278–13283

35. Franke, B., Akkerman, J. W. N., and Bos, J. L. (1997) *EMBO J.* **16,** 252–259
36. Blaukat, A., Ivankovic-Dikic, I., Gronroos, E., Dolfi, F., Tokiwa, G., Vuori, K., and Dikic, I. (1999) *J. Biol. Chem.* **21,** 14893–14901
37. Yan, Z., Feng, J., Fienberg, A. A., and Greengard, P. (1999) *Proc. Natl. Acad. Sci. U. S. A.* **96,** 11607–11612
38. Burgering, B. M. T., and Bos, J. L. (1995) *Trends Biol. Sci.* **20,** 18–22

cAMP-dependent Protein Kinase Induces cAMP-response Element-binding Protein Phosphorylation via an Intracellular Calcium Release/ERK-dependent Pathway in Striatal Neurons

Patrizia Zanassi, Mayra Paolillo, Antonio Feliciello, Enrico V. Avvedimento, Vittorio Gallo and Sergio Schinelli

---

Access the most updated version of this article at doi: 10.1074/jbc.M007631200

Alerts:

- When this article is cited
- When a correction for this article is posted

Click here to choose from all of JBC's e-mail alerts

This article cites 38 references, 16 of which can be accessed free at
http://www.jbc.org/content/276/15/11487.full.html#ref-list-1